Noninvasive Index of Cryorecovery and Growth Potential for Human Follicles In Vitro[1]

Susan L. Barrett,[3,4] Lonnie D. Shea,[5] and Teresa K. Woodruff[2,3]

Department of Obstetrics and Gynecology,[3] Northwestern University, Feinberg School of Medicine, Chicago, Illinois Center for Reproductive Science, Reproductive Biology Training Program[4] and Department of Chemical and Biological Engineering,[5] Northwestern University, Evanston, Illinois

ABSTRACT

Cryopreservation of oocytes and embryos is commonly used to preserve fertility. However, women undergoing cancer treatment may not have the time or may not be good candidates for these options. Ovarian cortical tissue cryopreservation and subsequent tissue transplant has been proven successful yet inefficient in preserving larger secondary follicles, and is not recommended as a fertility preservation option for women with certain cancers. We evaluated cryopreservation of individual follicles as an alternative option in rodents, nonhuman primates, and human primates. Under optimal conditions, cryopreserved mouse secondary follicles were able to reestablish granulosa cell-oocyte interactions, which are essential for subsequent follicle growth. Individual secondary follicles survived cryopreservation, were able to be cultured in a three-dimensional alginate hydrogel matrix to the antral stage, and the enclosed oocytes were competent for fertilization. Using a vital imaging technique (pol-scope) employed in many fertility centers, we were able to bioassay the thawed, cultured follicles for the presence of transzonal connections between the somatic and germ cells. Perturbations in these linkages were shown to be reversed when follicles were cryopreserved under optimal freezing conditions. We applied the optimized cryopreservation protocol to isolated rhesus monkey and human secondary follicles, and using the birefringent bioassay, we were able to show good correlation between early follicle growth and healthy somatic cell-oocyte connections. Our results suggest that ovarian follicles can be cryopreserved, thawed, and analyzed noninvasively, making follicle preservation an additional option for young cancer patients.

alginate, birefringence, cryopreservation, fertility preservation, follicle, transzonal projections

INTRODUCTION

Approximately 39 in 100 000 women under the age of 44 were diagnosed with cancer between 2002 and 2006, and of these women, 84% had a favorable prognosis (NCI SEER cancer statistics 2006). Unfortunately, many cancer therapies, such as alkylating agents and pelvic radiation, render women subfertile or infertile by damaging growing follicles and depleting follicular reserves [1]. Prior to cancer therapy, current fertility-sparing options for women include oocyte and embryo cryopreservation; however, women must delay treatment to undergo hormonal stimulation to obtain enough oocytes for in vitro fertilization or cryopreservation, and hyperstimulation may not be possible for women facing hormone-sensitive cancers or for young girls [2, 3]. Ovarian tissue cryopreservation is offered as an experimental option for fertility preservation prior to cancer treatment [4]. As of 2009, six babies have been born as a result of autotransplantation of cryopreserved tissue [5–8], and several more have been born after noncryopreserved or frozen heterologous transplants between monozygotic twins [9–11]. Successful ovarian tissue cryopreservation transplants use the outer 1 mm of ovarian cortex, which is rich in the immature primordial follicles that comprise the pool of follicles that enter the growing population over time. Unfortunately, the larger follicles, which include primary, secondary, and multi-layered secondary follicles, either are discarded prior to freezing or are destroyed in the cryopreservation/vitrification process [12–14]. Moreover, ovarian tissue collected before treatment may contain residual cancer cells; thus, cryopreservation of these immature follicles could be used either in transplant to minimize disease or for in vitro follicle growth with the goal of providing a mature gamete for fertilization.

Several studies have shown that either cryopreservation or vitrification of individual mouse follicles has resulted in live births; however, these cryopreservation protocols have not been tested on primate or human tissue [15–17]. Moreover, culture systems used to grow mouse follicles postthaw are two-dimensional systems [18] or three-dimensional culture systems [19, 20] that fail to support human follicle growth or antrum formation over an extended period of time. Previous reports in the mouse [21], nonhuman primate [22], and human [23] have shown that in-follicle maturation in a three-dimensional (3D) alginate-hydrogel matrix is capable of supporting follicle growth to generate mature oocytes competent for fertilization in vitro [21, 23]. The alginate hydrogel culture system provides an excellent tool for determining whether follicle and oocyte growth can be supported following individual follicle cryopreservation and thawing.

One of the challenges faced by the field is the development of tools that can assess follicle health immediately after cryothaw. Moreover, because human tissue is so rarely available for research, robust, noninvasive, vital technologies are urgently needed. Presently, in many fertility clinics the pol-scope is used to determine spindle location prior to intracytoplasmic sperm injection [24, 25], particularly after oocyte cryopreservation [26]. This technique also aids in spindle enucleation in the process of cloning [27]. Interestingly, the pol-scope has also been used to assess the thickness of the zona

pellucida in hamster embryos during assisted hatching [28]. We too elected to use the anatomically rich region of the zona pellucida as an opportunity to solve each of these methodological problems. The germ cell and the surrounding somatic cells must communicate throughout development and do so through transzonal projections (TZPs) that extend through the glycoprotein-rich zona pellucida and connect via gap junctions on the oocyte membrane. TZPs are essential for the bidirectional transport of molecules such as amino acids [29, 30], cAMP [31, 32], glucose [33], and pyruvate [34], which are essential for oocyte growth. Starting in the primordial follicle stage, TZPs form from initial, simple cell-cell gap junctions that are continuously remodeled and elongated during the formation of the zona pellucida and the course of oocyte growth [35]. Oocyte and follicle growth are dependent on the maintenance of these structures for survival, but because of their composition of F-actin and microtubules [36], they are very sensitive to changes in temperature and sheer stress, and are vulnerable during cryopreservation [12]. The TZP network is predicted to be a good biomarker of follicle health, because it is necessary for bidirectional communication between the somatic cells and the oocyte. Here, we assayed the quality of these connections in noncryopreserved and cryopreserved rodent, nonhuman primate, and human secondary follicles over time. We assessed the utility of a noninvasive microscopic technique (pol-scope), currently used in several clinics, for providing an in-depth measure of TZP integrity. Because destructive technologies are not suitable for application in the human setting, this bioassay provides a powerful new way to assign an early, noninvasive index of cryorecovery and growth potential for human oocytes postthaw.

MATERIALS AND METHODS

Animals

Immature follicles were isolated from prepubertal, 12- to 14-day-old female F1 hybrid (C57BL/6J × CBA/Ca) mice for both noncryopreserved and cryopreserved experiments. Sperm was prepared from proven CD1 male breeders. Animals were purchased (Harlan), housed in a temperature- and light-controlled environment (12 L:12 D), and provided with food and water ad libitum. Animals were fed Harlan Teklad Global irradiated 2919 chow, which does not contain soybean or alfalfa meal and therefore contains minimal phytoestrogens. Animals were treated in accordance with the NIH Guide for the Care and Use of Laboratory Animals, and protocols were approved by the Institutional Animal Care and Use Committee at Northwestern University.

Isolation and Growth of Mouse Follicles

Early secondary follicles (two to three granulosa layers) were isolated from 12- to 14-day-old mice and encapsulated into sterile 0.5% (w/v) alginate beads as described previously [37]. Ovaries were isolated into prewarmed collection medium (Liebovitz L-15; Invitrogen) containing 1 mg/ml bovine serum albumin (BSA) and 50 IU/ml penicillin/streptomycin (Invitrogen). For the cryopreserved follicle group, follicles were mechanically isolated using insulin gauge needles and were stored in L-15 medium prior to cryopreservation as described below. Upon thawing, follicles were stored in maintenance medium, α-MEM containing 1 mg/ml BSA and 50 IU/ml penicillin/streptomycin at 37°C, 5% CO_2 for 2 h prior to encapsulation in alginate hydrogel according to previously published methods [21]. Follicles were grown in α-MEM containing 1 mg/ml bovine fetuin (Sigma-Aldrich), 5 μg/ml insulin, 5 μg/ml transferrin, 5 ng/ml sodium selenite (Sigma-Aldrich), 3 mg/ml BSA, and 10 mIU recombinant human follicle-stimulating hormone (gift from Organon).

Isolation and Growth of Nonhuman Primate Follicles

Rhesus macaque ovaries (age 13 yr) were obtained from the laboratory of Dr. Leo Towle in the Department of Neurology at the University of Chicago under an approved material transfer agreement. All follicles in this study were collected from noncryopreserved tissue, which was cut into approximately 1-mm³ pieces in dissection medium (L-15 medium [Invitrogen] supplemented with 1% serum protein substitute [SPS, CooperSurgical], 100 IU/ml penicillin, and 100 mg/ml streptomycin [Invitrogen]). The tissue was then enzymatically digested by transferring it into dissection medium containing 0.2% collagenase and 0.02% DNase (Worthington Biochemical) for 30 min at 37°C in a shaking water bath. Follicles were mechanically isolated from the tissue strips using 25-gauge needles, transferred to maintenance medium (α-MEM [Invitrogen] supplemented with 1% SPS, 100 IU/ml penicillin, and 100 mg/ml streptomycin), and placed in an incubator at 37°C and 5% CO_2 for 2–6 h prior to encapsulation (noncryopreserved controls) or cryopreservation. Follicles were grown in α-MEM containing 1 mg/ml bovine fetuin (Sigma-Aldrich), 5 μg/ml insulin, 5 μg/ml transferrin, 5 ng/ml sodium selenite (Sigma-Aldrich) and 3 mg/ml BSA. No FSH was added to these cultures.

Isolation and Growth of Human Follicles

Portions of four patients' ovarian tissue (never more than 20% of the total) were donated for research following informed consent under an IRB-approved protocol at Northwestern University. All follicles included in this study were collected from noncryopreserved tissue, which was cut into approximately 1-mm³ pieces in dissection medium (L-15 medium; Invitrogen) supplemented with 1% SPS (CooperSurgical), 100 IU/ml penicillin, and 100 mg/ml streptomycin (Invitrogen). Human follicle isolation and culture is followed exactly as rhesus follicle isolation and culture at this point.

Cryopreservation and Thawing of Follicles

After individual follicles were isolated from ovarian tissue, they were washed in collection medium 2 times before transferring to 1 ml cryopreservation medium (~30 follicles per tube) containing L-15 medium, sucrose 35 mg/ml (final concentration), Quinns Advantage SPS (Cooper-Surgical) 10% (v/v), and ethylene glycol 8.83% (v/v) for 30 min at room temperature followed by 30 min at 4°C. Follicles were then transferred to cryotubes containing 1 ml of prechilled cryoprotectant for 10 min.

The tubes were then transferred to a 4°C freeze-control Cryobath (CryoLogic). Cryopreservation was controlled by CryoGenesis V software (CryoLogic), which cooled the tubes to −7°C at a rate of 2°C/min. Cryoseeding was performed at −7°C (permissive temperature; the ideal temperature for crystallization seeding for secondary follicles in ethylene glycol) or −9°C (nonpermissive/negative control), followed by chilling to −40°C at 0.3°C/min and then storage in liquid nitrogen until thawing.

For thawing, tubes of follicles were removed from N_2 (l) and held at room temperature for 30 sec prior to being submerged in a 37°C water bath for 2.5 min. Contents of the cryotube were removed using a trimmed 1-ml pipet tip and placed in a 60-mm culture dish. Retrieved follicles were transferred to room temperature L-15 medium containing 10% SPS and sucrose 35 mg/ml for 3 × 10 min with decreasing amounts of ethylene glycol (5.57%, 2.79% and 0% [v/v]). Follicles were then transferred to a dish of room temperature L-15 medium containing 10% SPS. The dish was put on a 37°C warming plate for 10 min before the follicles were transferred to maintenance medium. Approximately 4–6 rounds of cryopreservation were carried out for each seeding temperature and tissue type.

Fixation and Immunofluorescence

Follicles to be imaged were fixed in 4% paraformaldehyde at 37°C for 1 h followed by storage in wash buffer [38]. Follicles were stained for F-actin by incubation in rhodamine-phalloidin (1:50; Invitrogen) and 1 μg/ml Hoechst (Invitrogen) overnight at 4°C. Follicles were washed 3 × 10 min in wash buffer prior to mounting in buffer containing saline/glycerol (1:1) and sodium azide 25 mg/ml. In order to maintain the three-dimensionality of the follicles during imaging, glass shards and wax were placed beneath the glass coverslip to prevent compression.

Confocal Microscopy and Line-Scan Analysis

Follicles were imaged on a Leica SP5 confocal microscope with a 40× oil objective. Full z-stacks images are comprised from 0.3 μm optical sections were completed for each follicle (n = 10 for each treatment group). Using Leica analysis software, four-pixel lines were drawn throughout the zona pellucida around the oocyte, in a 0.3-μm optical section, in order to determine the frequency (number of TZPs per 10-μm segment surrounding the oocyte). Three independent line scans were completed on five different sections per follicle (totaling 15 line scans per follicle).

Birefringence Analysis

To quantify the maintenance of TZPs throughout the zona pellucida in noncryopreserved and cryopreserved follicles, we used the Abrio Imaging System (CRi), which detects birefringent properties of cells. Birefringence is an
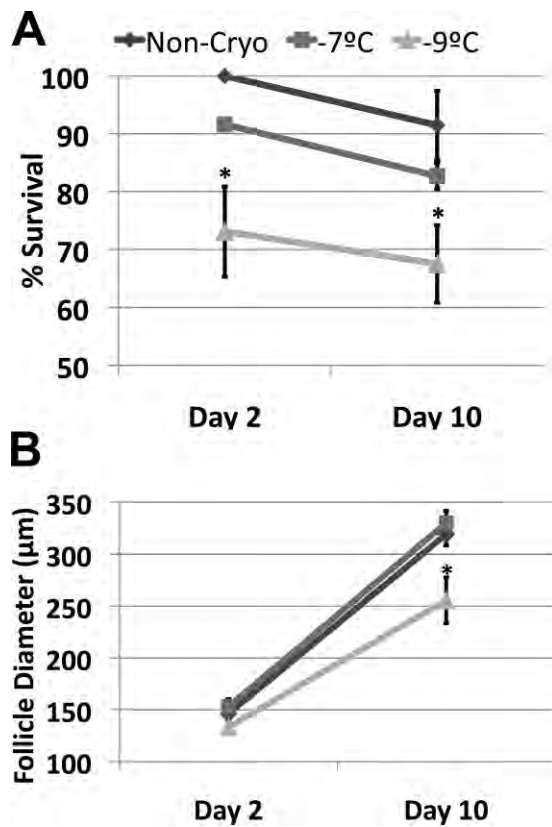
FIG. 1. **A**) Survival in noncryopreserved (Non-Cryo) and cryopreserved (with seeding temperatures of −7°C and −9°C) follicles over a 10-day culture period. Error bars represent ± SEM. *$P < 0.05$. **B**) Growth of noncryopreserved and cryopreserved follicles between Day 2 and Day 10 of culture. Error bars represent ± SEM. *$P < 0.01$.

intrinsic property of a sample that contains molecular order and can be detected by a polarized light microscope (Pol-scope; Cambridge Research & Instrumentation, Inc., Oosight Imaging Systems, Woburn, MA), and is measured by differences in polarized light as the retardance value [39]. The Abrio system was customized for our inverted Nikon Eclipse TE-300. Birefringence was analyzed using 20× and 40× Plan Fluor DIC objectives. The Abrio software was capable of determining the orientation as well as the retardance value of the birefringence properties.

Microinjection and Dye Tracking

Twenty-five noncryopreserved (Day 0 after isolation and Day 2 of culture) and 25 cryopreserved (Day 0 immediately after thaw and Day 2 of culture) C57BL/6J × CBA/Ca two- to three-layer secondary follicles were injected with 10% Lucifer yellow CH, lithium chloride (L12926; Invitrogen) in EmbryoMax Injection Buffer (Chemicon; Millipore) as previously described [40, 41]. Injections into the oocyte were made using MicroJek EggJek injection needles (0.5-μm inner diameter) for 1 sec at 120 hPa, and the dye was allowed to transfer to the surrounding granulosa cells via gap junctions for 10 min before being imaged on a Leica SP5 confocal microscope fitted with a resonance scanner. In order to assess the gap junction-TZP coupling, 10 Lucifer yellow fluorescent intensity measurements (0–255 units) were taken per follicle in the area of the granulosa cells. Two intensity measurements were taken every fifth section on 0.3-μm optical slices. The average intensity was then plotted against the average number of TZPs per 10 μm for each treatment and time point. All data was collected on and analyzed on a Leica TCS SP5 resonance scanning confocal microscope with Leica LAS AF software.

Statistical Analysis

TZP counts and retardance measurements from control (noncryopreserved) follicles and follicles pre- and postcryopreservation and thaw were subjected to one-way analysis of variance followed by Bonferroni multiple comparison post hoc test to determine the significance of each treatment group using Prism 4 (GraphPad Software). Calculated values are shown ±SEM with a significance

level of $P < 0.05$ being considered significant. Retardance measurements from follicles pre- and postcryopreservation and thaw were plotted in box and whisker plots to represent the median value, minimum and maximum values, and upper and lower quartiles.

RESULTS

Growth and Survival of Noncryopreserved and Cryopreserved Mouse Follicles

As a control against which we could evaluate the successful cryopreservation and thawing of individual ovarian follicles, we first analyzed the growth characteristics of noncryopreserved follicles grown in the 3D alginate hydrogel culture system. Two-layered secondary follicles were isolated and cultured for 10 days, and immunofluorescent images were taken every 2 days to identify healthy and unhealthy/dead follicles. After 2 days, 100% of cultured follicles were healthy (Fig. 1A), with intact basement membranes and healthy, visible oocytes (not shown). By 10 days, 91.5 ± 5.96% of follicles were healthy and had grown from ~150 μm to 319 ± 11.1 μm in diameter (Fig. 1B).

Because mouse follicles progress well to terminal maturation, we used two seeding temperatures to more rigorously test the assay's ability to detect the correlation between TZPs and follicle health. Follicles were cryopreserved at two seeding temperatures, −7°C (permissive) and −9°C (nonpermissive), based on previously validated seeding temperatures for ethylene glycol in embryo and ovarian tissue cryopreservation [42–44]. After thawing, follicles were encapsulated in alginate and cultured for 10 days, with survival assessed every 2 days. It was found that the 2-day survival rate for follicles seeded at the permissive temperature was approximately 91.6 ± 0.60%, compared with the survival rate for follicles seeded at the nonpermissive temperature (73.1 ± 7.81%; Fig. 1A). At 10 days of culture, follicles seeded at −7°C had a much higher survival rate (82.7 ± 2.29%) than follicles seeded at −9°C (67.5 ± 6.67%; Fig. 1A). Accordingly, it was found that follicles seeded at −7°C grew in diameter from an average of 153 ± 7.38 to 330 ± 11.7 μm, which was a statistically ($P < 0.01$) larger increase than that seen in follicles seeded at the nonpermissive temperature (from 133 ± 3.52 to 255 ± 22.2 μm; Fig. 1B).

Analysis of TZPs in Cryopreserved Mouse Follicles

Because follicle growth and survival is dependent on communication between the granulosa cells and the oocyte via TZPs, we determined whether TZPs survived the cryopreservation process or were capable of regrowth after cryopreservation and thawing. A selection of cultured follicles (both noncryopreserved and cryopreserved) were fixed on Days 0, 2, 6 and 10 during the culture period and stained to examine the organization of TZPs in the area of the zona pellucida by confocal microscopy (Fig. 2A).

Noncryopreserved two-layer secondary follicles contained, on average, eight TZPs per 10 μm of zona space surrounding the oocyte (Fig. 2B). At 2 and 6 days of culture, TZPs in noncryopreserved follicles increased to 11 per 10 μm, and by Day 10, there were 12 TZPs per 10 μm (Fig. 2B). Immediately thawed follicles showed few TZPs, with four and two TZPs per 10 μm for follicles seeded at −7 and −9°C, respectively. At Day 2, TZPs increased to nine (−7°C) and three (−9°C) TZPs per 10 μm. By 10 days of culture, TZPs in follicles seeded at the nonpermissive temperature increased to eight TZPs, whereas TZPs in follicles seeded at −7°C increased to 11 per 10-μm section of zona (Fig. 2B).
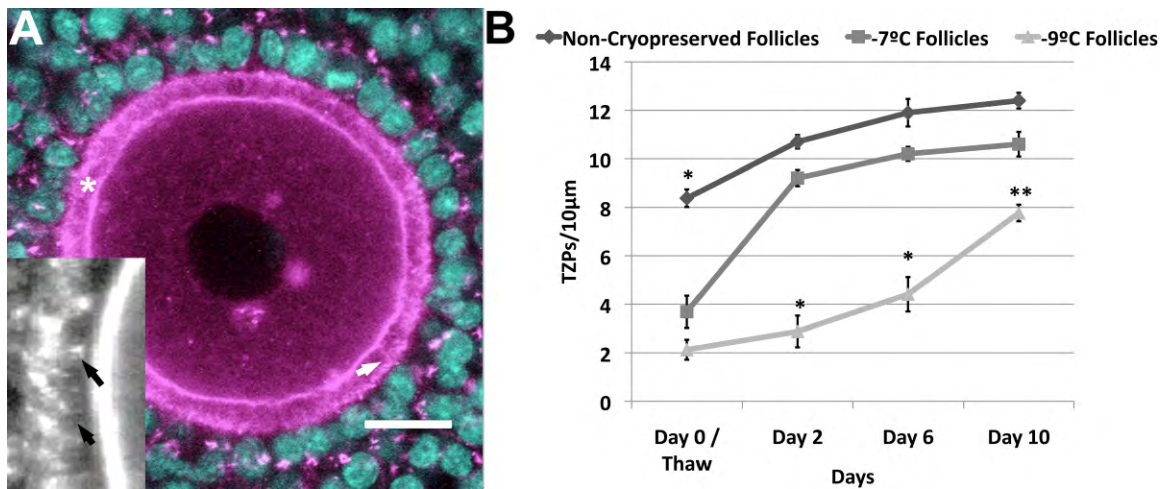
FIG. 2. **A**) TZP frequency is recorded for every 10 μm around the follicle perimeter in the area of the zona pellucida (*). F-actin (purple), DNA (blue-green). Bar = 20 μm. Inset shows an enlarged area of the zona depicting individual TZPs from one 0.3-μm section of the full Z-stack. Arrows depict individual TZPs. **B**) TZP frequency in noncryopreserved and cryopreserved cultured mouse follicles over a 10-day culture period. Error bars represent ± SEM. *$P < 0.001$, **$P < 0.01$.

After 10 days of culture, follicles were stimulated for 16 h to induce in vitro maturation, and then the oocytes were examined for resumption of meiosis. It was found that 93% (n = 67) of oocytes from noncryopreserved follicles, 57.3% (n = 35) of oocytes in the −7°C group, and 30.7% (n = 21) of oocytes from the −9°C group matured to the MII stage. MII-staged oocytes were subjected to in vitro fertilization and were examined for pronuclear formation after 6 h. It was found that 79% (n = 53) of oocytes from the noncryopreserved group, 57% (n = 20) from the −7°C group, and 52% (n = 11) from the −9°C group were able to be fertilized and form pronuclei.

Functional TZP Studies

To assess the functionality of the TZPs in noncryopreserved and cryopreserved mouse follicles (2 h after thawing), Lucifer yellow was injected into the oocytes of noncryopreserved and cryopreserved follicles and the ability of the dye to transfer from the oocyte to the surrounding granulosa cells through intact gap junctions was examined. After 10 min, the follicles were imaged for dye transfer by confocal microscopy (Fig. 3). Injected noncryopreserved follicles contained brightly stained oocytes surrounded by several stained granulosa cells indicative of intact gap junctions (Fig. 3A, a). After 2 days of culture, isolated, noncryopreserved follicles were injected and shown to transfer dye to surrounding somatic cells (Fig. 3B, b). In cryopreserved follicles, immediately after thawing, no dye transferred from the oocyte to the surrounding granulosa cells (Fig. 3C, c). However, after 2 days in culture, follicles cryopreserved at −7°C were injected and were able to transfer Lucifer yellow dye to surrounding granulosa cells, indicating the reformation of TZPs and gap junctions (Fig. 3D, d); very little dye transferred in follicles cryopreserved at a seeding temperature of −9°C after 2 days of culture (3E, e).

Though it was determined that TZPs were reestablished and functional by the passage of Lucifer yellow dye from the oocyte to the granulosa cells in −7°C follicles, it was necessary to establish the coupling strength of the gap junctions at the ends of TZPs in these follicles (Fig. 4). The amount of dye transferred to the granulosa cells was quantified by the average fluorescent intensity per 0.3-μm section and was plotted against the average number of TZPs per 0.3-μm section. It was found that noncryopreserved follicles were moderately coupled on the day of isolation, having an average of nine TZPs and an average fluorescent intensity of 60 units. However, after 2 days in culture, the TZPs and gap junctions were highly coupled, increasing to 11 TZPs and 110 fluorescent units. Analysis of thawed follicles showed very little initial coupling of gap junctions and TZPs. Interestingly, after 2 days in culture, follicles cryopreserved with a seeding temperature of −7°C increased in gap junction-TZP coupling, whereas follicles cryopreserved with a seeding temperature of −9°C did not. Overall, the number of TZPs directly correlated with the average fluorescent intensity of dye.

Analysis of TZPs Using Birefringence Analysis

In order to avoid terminal assessment of follicle health, we wanted to test whether noninvasive polarized light is capable of detecting TZPs vitally in growing follicles, as a biomarker of follicle health. Therefore, we investigated an alternative technique of birefringence analysis, which is used to detect organized microtubules and F-actin in living cells [39]. We first investigated whether a pol-scope was able to detect the organized proteins of the zona pellucida and TZPs by comparing the birefringence of the zona pellucida region of untreated mouse follicles (Fig. 5A) and of follicles treated with latrunculin B, an actin depolymerizer (Fig. 5B). In the untreated follicles, birefringence is seen around the oocyte in Figure 5A (inset, birefringence alone) and is absent from the images of follicles treated with actin depolymerizers for 5 h (Fig. 5B; inset, birefringence alone). Birefringence measurements in the area of the zona were recorded, and revealed that treating follicles with latrunculin B significantly decreased the retardance to 1.3 nm compared with 2.25 nm in untreated follicles (Fig. 5E). Untreated and latrunculin B-treated follicles were fixed and prepared for confocal microscopy to image TZPs. Control follicles showed intact TZPs throughout the zona pellucida (Fig. 5C), which had approximately 8.9 ± 0.25 TZPs per 10 μm. As expected, follicles treated for 5 h with latrunculin B displayed depolymerized actin bundles in the area of the zona (Fig. 5D), containing 3.6 ± 0.37 TZPs per 10 μm. From this assessment, we can conclude that in mouse follicles, birefringence of the zona pellucida occurs at levels <1.0 nm, and signals >1.0 nm represent birefringence of TZPs.
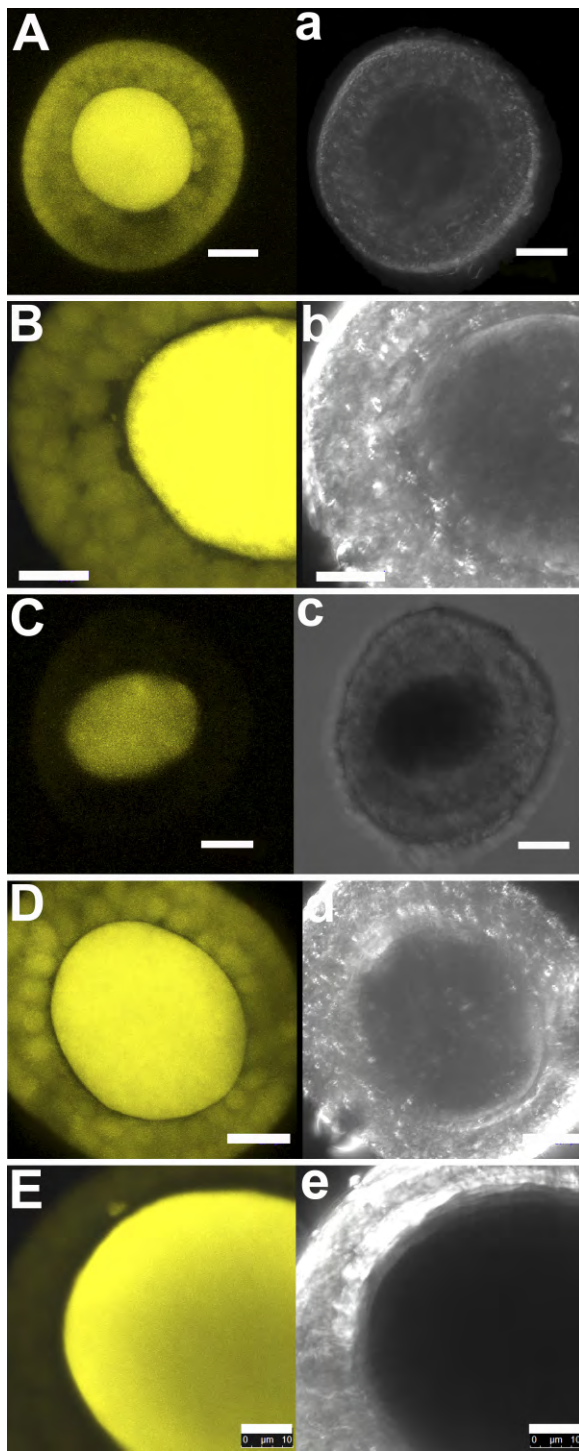
FIG. 3.   Microinjection of Lucifer yellow tracking dye to detect functional TZPs and gap junctions in Day 0 (**A**, **a**) and Day 2 (**B**, **b**) noncryopreserved follicles, Day 0 (**C**, **c**) and Day 2 (**D**, **d**) cryopreserved follicles seeded at −7°C, and Day 2 (**E**, **e**) cryopreserved follicles seeded at −9°C. Brightfield images are shown in lowercase-labeled panels. Bars = 25 μm (**A**, **a**, **C**, **c**), 15 μm (**B**, **b**) and 20 μm (**D**, **d**).

FIG. 4.   Coupling strength of TZPs to gap junctions in noncryopreserved (NC) and cryopreserved follicles. The average TZP number per 10 μm and the average fluorescent intensity of Lucifer yellow in the granulosa cells shows that gap junctions are highly coupled in noncryopreserved follicle. Immediately after thawing, gap junctions and TZPs are not coupled in −7°C and −9°C. However, after 2 days in culture gap junction-TZP coupling has increased in −7°C, yet in −9°C it has not. Error bars represent ± SEM. a Represents $P < 0.01$ between −7°C and −9°C on the same day. b Represents $P < 0.01$ between −7°C and $P < 0.001$ between −9°C on same day. c Represents $P < 0.01$ between −9°C on same day.

We then analyzed the birefringence properties of non-cryopreserved and cryopreserved follicles during culture in alginate. All two-layer secondary follicles recorded similar retardance levels prior to freezing, ranging from 1.75 to 2.2 nm (Fig. 6). Noncryopreserved follicles continued to increase in birefringence throughout the 6 days of culture to 2.75 nm, consist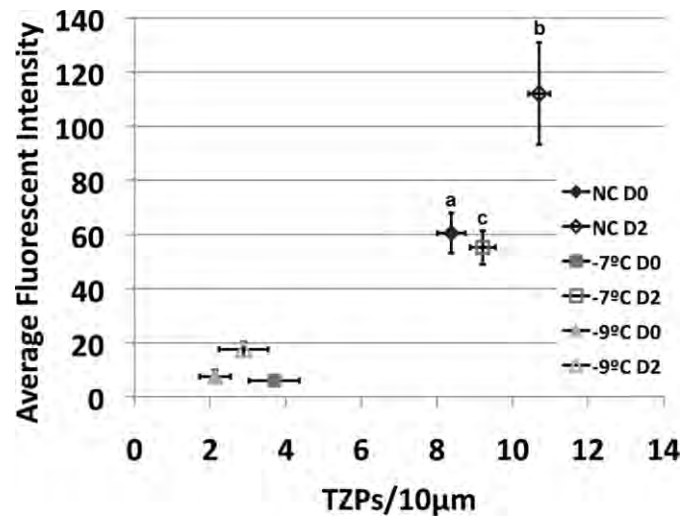ent with the increase in TZPs during this culture period (Fig. 2B). After thawing, Day 0 cryopreserved follicles showed a decrease in retardance to 1.0 nm; however, by Day 2 of culture, follicles cryopreserved at the permissive seeding temperature showed an increase to 2.0 nm, consistent with the regrowth in TZPs seen in Figure 2B, and by Day 6, these follicles increased retardance to 2.5 nm. However, follicles cryopreserved at the nonpermissive seeding temperature failed to significantly increase levels of retardance throughout the 6-day culture period, ending at 1.25 nm (Fig. 6).

Cryopreservation of Nonhuman Primate Follicles

To determine whether cryopreservation of individual follicles can be applied to human fertility preservation, and to test whether the birefringence assay is adaptable to assessing follicle health in other species, we isolated individual secondary follicles from rhesus macaques and analyzed their follicle growth characteristics in alginate culture as well as the birefringent properties of their TZPs.

Isolated follicles were less than 200 μm in diameter and increased to 350 μm during 6 days of culture (Fig. 7A). Interestingly, the birefringence properties of noncryopreserved rhesus follicles were consistent throughout the growth period, ranging from 3 to 4 nm (Fig. 7B). Cryopreserved follicles (using the permissive seeding temperature) were approximately 175 μm in diameter after thawing and grew to over 250 μm during 6 days of culture (Fig. 7C). The birefringent properties of cryopreserved rhesus follicles could be detected using a pol-scope, with precryopreservation retardance values of approximately 2.75 nm. Following thaw (postcryopreservation), values decreased on average to 1.25 nm. By 2 days of culture, however, the retardance values increased to approximately 3.0 nm, which was maintained throughout the 6-day culture period (Fig. 7D), consistent with values seen in Figure 7B. On Day 6, both noncryopreserved and cryopreserved follicles were fixed and assessed for TZPs; they contained 17.1 ± 0.51 (Fig. 7E) and 14.3 ± 0.83 TZPs per 10 μm, respectively.

FIG. 6. Analysis of the birefringent properties of noncryopreserved (NC) and cryopreserved mouse follicles cultured for 6 days. Fresh follicles show an increasing retardance over 6 days of culture. Cryopreserved follicles showed a decrease in retardance after cryopreservation at the permissive temperature but an increase back to noncryopreserved levels after 2 days in culture. Error bars represent ± SEM. *$P < 0.01$, **$P < 0.001$ between treatment groups on the same day.
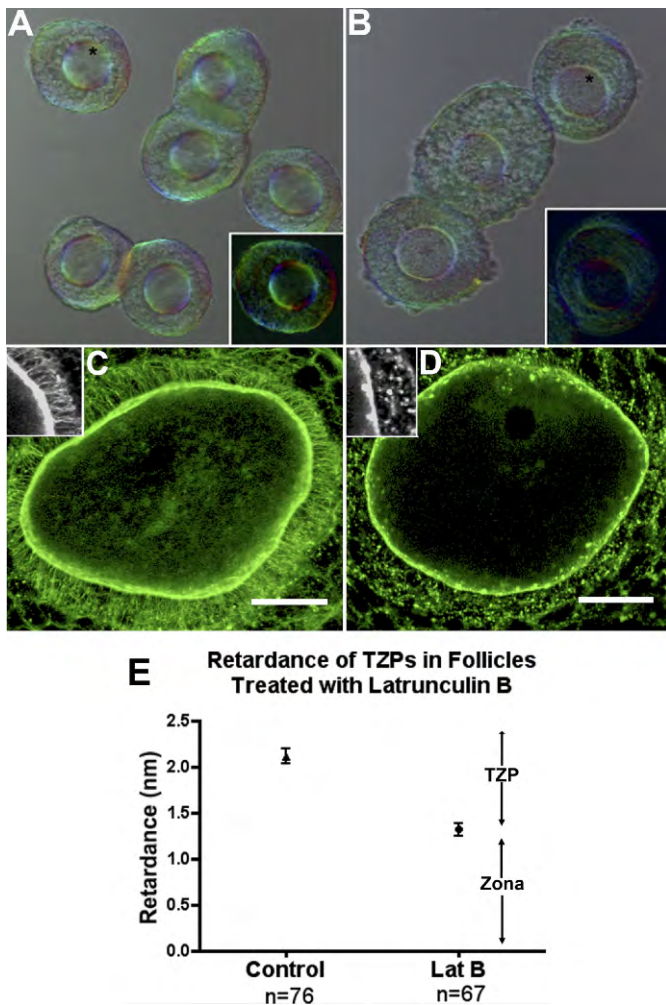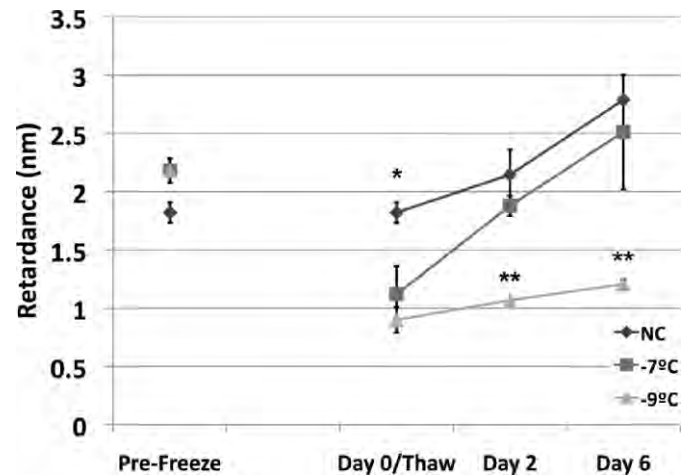
FIG. 5. Birefringence analysis of TZPs in follicles treated with the actin depolymerizing drug latrunculin B. Birefringent images of untreated follicles (**A**) and follicles after 5 h of latrunculin B (Lat B) treatment (**B**); follicle diameter is 150 μm. Insets represent birefringence of the cell marked with asterisks (*). Confocal image of a 5-h control follicle stained for F-actin (green) to show transzonal projections (**C**, inset). Confocal image of a follicle treated for 5 h with latrunculin B and stained for F-actin (green) showing no transzonal projections (**D**, inset). Bars = 25 μm. **E**) Nontreated follicles have a much higher retardance than follicles treated for 5 h with 250 μM latrunculin B. A retardance score below 1.0 nm represents birefringence from the zona and a retardance score above 1.0 nm represents birefringence from TZPs. Error bars represent ± SEM.

Cryopreservation of Human Follicles

It has been established that TZPs are reflective of birefringence in mice (Fig. 5), and rhesus follicles show numerous TZPs (Fig. 7E), which associate with high levels of birefringence (Fig. 7B). Therefore, we lastly examined the health of noncryopreserved and cryopreserved follicles from four human oncofertility patients to determine if birefringence from human follicles, as shown by the bright birefringent ring in the area of the zona (Fig. 8A), positively correlates with follicle growth and health. Noncryopreserved follicles were grown for 6 days in the alginate culture system. Diameter and birefringence were plotted for each individual follicle (Fig. 8C). Follicle sizes ranged from 80 to 425 μm in diameter, with retardance ranging from 1.5 to 5.25 nm. Noncryopreserved follicles were found to have a positive correlation between increased follicle diameter and high levels of birefringence. Though cryopreserved human follicles displayed little birefrin-

gence immediately following thaw (Fig. 8B), follicles were capable of reestablishing physical connections. Data from cryopreserved follicles (−7°C seeding temperature) were also plotted according to follicle diameter and retardance value (Fig. 8D). Follicles ranged from 80 to 175 μm in diameter and had retardance values from 0.75 to 2.5 nm. Cryopreserved human follicles were also found to have a positive correlation between follicle growth and an increase in birefringence (Fig. 8D). On Day 6 of culture, fixed-follicle analysis revealed that noncryopreserved and cryopreserved follicles contained 11.3 ± 0.34 and 7.0 ± 0.58 TZPs per 10 μm, respectively.

DISCUSSION

Understanding the impact of cryopreservation of secondary ovarian follicles not only allows researchers an opportunity to study the importance of granulosa cell-oocyte communication for follicle survival, it also holds potential for expanding fertility preservation options for women facing fertility-threatening diseases or treatments, and improving methods of preserving tissue of endangered species. Various groups have studied cryopreservation of ovarian tissue as well as the preservation of oocytes and embryos; however, we believe this is the first study to examine the importance of preserving the connectivity between the granulosa cells and the oocyte after cryopreservation. Here we report that 1) individual secondary follicles (mouse, rhesus monkey and human) may be cryopreserved and grown in a 3D matrix; 2) successful follicle growth following cryopreservation correlates with the ability of follicles to reestablish and remodel TZPs; and 3) vital detection of TZPs via birefringence is a reflection of follicle health and can be detected following cryopreservation.

Follicle Growth and Survival Postcryopreservation

Secondary follicles in situ fail to survive the cryopreservation process because of ice formation in the large fluid volumes of the oocyte and follicle, as well as poor penetration of the cryoprotectant [45]. We hypothesized that isolation from ovarian cortical tissue and cryopreservation of individual preantral secondary follicles would increase the follicle

FIG. 7. Growth and birefringent properties of noncryopreserved and cryopreserved rhesus monkey follicles. **A**) Increased growth of noncryopreserved follicles during 6 days in culture. **B**) The birefringent properties of fresh follicles did not change during 6 days in culture and maintained retardance values between 3 and 4 nm. **C**) Growth of cryopreserved follicles after 6 days in culture. **D**) Birefringence of cryopreserved follicles showed a decreased retardance after cryopreservation and an increased retardance to noncryopreserved levels after 2 days in culture. **E**) Staining of TZPs (green) in a noncryopreserved rhesus follicle, DNA (red). Box plot graphs represent the median value and minimum and maximum values as well as the upper and lower quartiles. Mean ± SEM marked with different lowercase letters are significantly different ($P < 0.05$) between culture days. Bar = 20 µm.
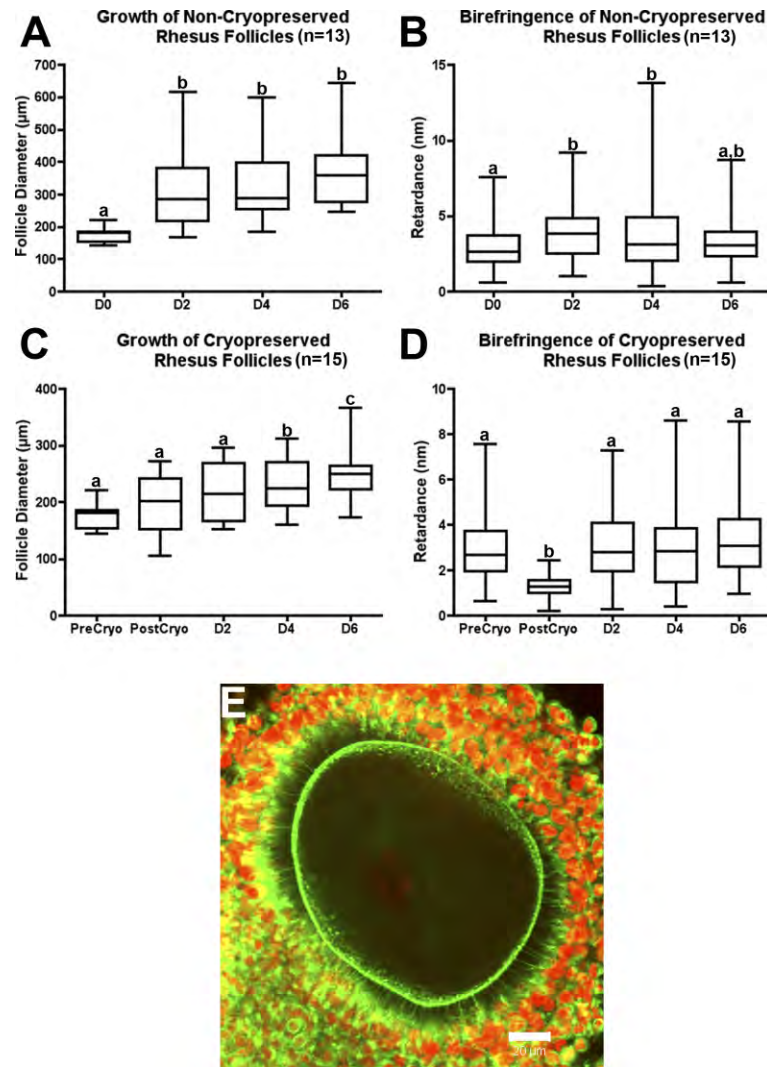
survival rate after thawing. Our group has previously demonstrated the ability to culture mouse [21], rhesus macaque [22], and human [23] secondary follicles in 3D alginate hydrogels, which is an essential step for resuming follicle growth after the cryopreservation process. Using this alginate hydrogel as a 3D matrix for follicle growth, we were able to assess the follicle health and growth following cryopreservation. Using a permissive ($-7°C$) seeding temperature for ethylene glycol, follicles survived the cryopreservation process and grew in culture for 10 days to a size comparable to noncryopreserved cultured follicles. We were also able to induce oocyte maturation in situ and fertilize MII oocytes from individual cryopreserved follicles, indicating that the zona pellucida did not lose its ability to interact and bind sperm. Rhesus monkey and human follicles were also individually cryopreserved and their growth characteristics were compared to noncryopreserved follicles. Although it was found that both rhesus monkey and human cryopreserved follicles grew more slowly following cryopreservation, they continuously increased follicle diameter during the entire culture period.

TZP Remodeling in Cryopreserved Follicles

In addition to being critical for bidirectional communication, it has been reported that TZPs play a role in maintaining the organization of the oocyte cortex in mice [46]. TZPs, which are primarily made of F-actin and form during the course of follicle development, are extremely sensitive to fluctuations in temperature [47–49] and are therefore as vulnerable as oocytes with regard to the destruction of the microtubule and actin network during the cryopreservation process [50]. Therefore, to best protect secondary follicles from the adverse cryo-effects on microtubules and microfilaments, follicles were individually isolated for better permeation of cryoprotectant.

Our confocal analysis of TZPs after cryopreservation showed that a large percentage of the physical connections in mouse follicles were destroyed after the thawing process but that they were capable of reconnecting in the 3D culture system; TZPs increased in number as the follicle increased in diameter during the first 6 days of culture. Follicles that were cryopreserved at the nonpermissive seeding temperature ($-9°C$) were unable to reestablish and maintain connectivity following cryopreservation, ultimately resulting in follicle death (seen in Fig. 1A). This highlights the importance of seeding temperature in the slow cryopreservation process. TZPs were also shown to be functional by the injection and transport of Lucifer yellow from the oocyte into the surrounding granulosa cells over 2 days of culture. Immediately after thawing, follicles were unable to transfer dye into surrounding granulosa cells, indicating either that TZPs were not present or that gap junctions were not functional. However, after 2 days of culture, cryopreserved follicles ($-7°C$) were able to reestablish TZPs and gap junctions and transport dye from
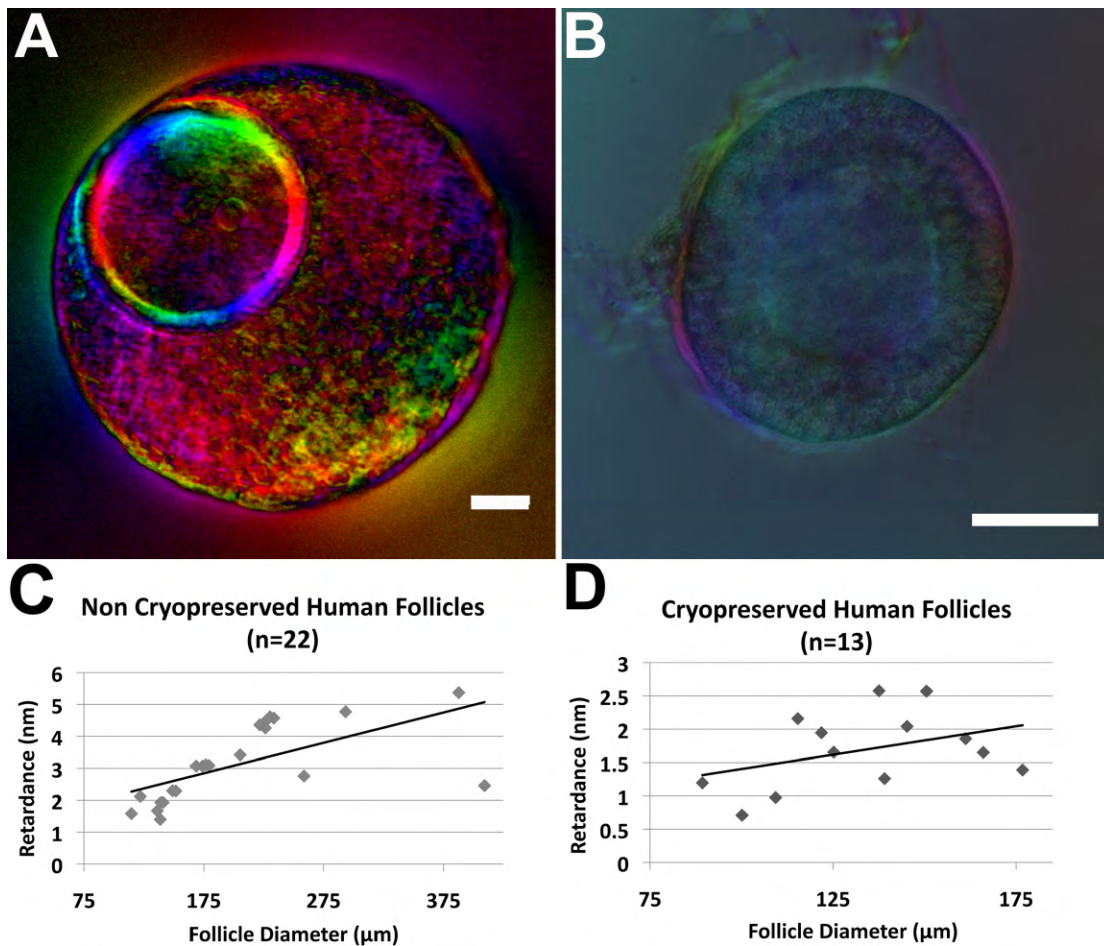
FIG. 8. Growth and birefringent properties of noncryopreserved and cryopreserved human follicles. **A**) Birefringent image of a human follicle grown for 6 days in alginate hydrogel; high levels of retardance are seen in the area of the zona. **B**) Birefringent image of a human follicle; note the lower levels of retardance are seen in the area of the zona. Colors represent directionality of the actin fibers. Bars = 30 μm (**A**) and 50 μm (**B**). Analysis of TZP retardance and follicle diameter in noncryopreserved follicles (**C**) and cryopreserved follicles (**D**). Regression lines show a positive trend for both noncryopreserved (y = 0.0095x + 1.183, R^2 = 0.3913) and cryopreserved follicles (y = 0.0085x + 0.5512, R^2 = 0.15243).

the oocyte into the surrounding somatic cells. This is the first report to establish that TZPs are able to regrow and function in follicles that have been cryopreserved.

Birefringence Analysis

Oocyte and embryo quality are assessed, both in the laboratory and the clinic, by several visual characteristics, such as the placement of the spindle and polar body and cleavage rate of blastomeres [51, 52]. However, the only way to vitally assess follicle health is by monitoring follicle growth and hormone secretion over several days [21–23]. We tested the effectiveness of an alternative vital assay of follicle health that uses a pol-scope to detect birefringence in the area of TZPs (zona pellucida). Microtubules and actin filaments, which are predominant components of TZPs, are organized structures that are easily detected by the pol-scope, similar to the microscopes used to detect the MII spindle in fertility clinics and transgenic labs [53–55].

We first tested the effectiveness of the polarized-light microscope to detect TZPs by depolymerizing actin filaments in follicles using latrunculin B. Treated follicles had a reduced number of TZPs per 10 μm and a concomitant reduction in birefringence in the area of the TZPs, a phenomenon that was not seen in untreated control follicles. It was established that the zona pellucida has an intrinsic birefringence level of 1.0

nm; additional birefringence above 1.0 nm is contributed by TZPs. Using the pol-scope on both noncryopreserved and cryopreserved growing mouse follicles in culture, the number of TZPs increased and decreased (Fig. 2B) in correlation with increases and decreases in birefringence (Fig. 6). The assessment of rhesus monkey and human follicles further validated the effectiveness of this vital assay on measuring the health of follicles (Figs. 7 and 8). It was found that both noncryopreserved and cryopreserved rhesus monkey follicles grew over a 6-day culture period and maintained high levels of birefringence, even after cryopreservation, which was consistent with high TZP counts seen on the last day of culture. Noncryopreserved and cryopreserved human follicles were assessed for health by examining follicle diameter and retardance values during 6 days of culture. Both noncryopreserved and cryopreserved follicles indicated that follicle size directly correlates with an increase in retardance, which is reflective of follicle health. Though cryopreserved follicles showed less of an increase in follicle size and birefringence over the course of the 6-day culture period, which may be a result of cryopreservation, we are still able to vitally assess follicle health using this method. This bioassay provides the badly needed technique that can immediately, systematically, and noninvasively monitor early follicle health after a cryopreservation insult. As new cryo-technologies emerge,

this method provides a signature endpoint that can be exploited routinely.

Our studies reveal that mouse, monkey, and human follicles are capable of surviving current cryopreservation techniques and that follicle health can be evaluated by a noninvasive imaging technique that detects intact TZPs. This technique may permit selection of healthy cryopreserved follicles that can then be encapsulated in a 3D alginate hydrogel matrix and grown in culture to produce healthy oocytes. By enriching the cultured follicle population in this way, we would expect to achieve higher rates of follicle survival and growth as well as higher rates of oocyte maturation and fertilization. The next challenge will be to determine how long nonhuman primate and human follicles can be cultured after cryopreservation, and to incorporate our vital assay into the 30-day primate and human follicle culture protocol [22, 23] to assess follicle and oocyte health over time.

ACKNOWLEDGMENTS

REFERENCES

1. Agarwal SK, Chang RJ. Fertility management for women with cancer. In: Woodruff TK, Snyder KA (eds.), Oncofertility: Fertility Preservations for Cancer Survivors. New York: Springer; 2007:15–26.
2. Brinton L. Long-term effects of ovulation-stimulating drugs on cancer risk. Reprod Biomed Online 2007; 15:38–44.
3. Azim AA, Costantini-Ferrando M, Oktay K. Safety of fertility preservation by ovarian stimulation with letrozole and gonadotropins in patients with breast cancer: a prospective controlled study. J Clin Oncol 2008; 26:2630–2635.
4. Jeruss JS, Woodruff TK. Preservation of fertility in patients with cancer. N Engl J Med 2009; 360:902–911.
5. Donnez J, Dolmans MM, Demylle D, Jadoul P, Pirard C, Squifflet J, Martinez-Madrid B, van Langendonckt A. Livebirth after orthotopic transplantation of cryopreserved ovarian tissue. Lancet 2004; 364:1405–1410.
6. Meirow D, Levron J, Eldar-Geva T, Hardan I, Fridman E, Zalel Y, Schiff E, Dor J. Pregnancy after transplantation of cryopreserved ovarian tissue in a patient with ovarian failure after chemotherapy. N Engl J Med 2005; 353:318–321.
7. Demeestere I, Simon P, Emiliani S, Delbaere A, Englert Y. Fertility preservation: successful transplantation of cryopreserved ovarian tissue in a young patient previously treated for Hodgkin's disease. Oncologist 2007; 12:1437–1442.
8. Andersen CY, Rosendahl M, Byskov AG, Loft A, Ottosen C, Dueholm M, Schmidt KL, Andersen AN, Ernst E. Two successful pregnancies following autotransplantation of frozen/thawed ovarian tissue. Hum Reprod 2008; 23:2266–2272.
9. Silber SJ, Lenahan KM, Levine DJ, Pineda JA, Gorman KS, Friez MJ, Crawford EC, Gosden RG. Ovarian transplantation between monozygotic twins discordant for premature ovarian failure. N Engl J Med 2005; 353:58–63.
10. Silber SJ, DeRosa M, Pineda J, Lenahan K, Grenia D, Gorman K, Gosden RG. A series of monozygotic twins discordant for ovarian failure: ovary transplantation (cortical versus microvascular) and cryopreservation. Hum Reprod 2008; 23:1531–1537.
11. Silber SJ, Gosden RG. Ovarian transplantation in a series of monozygotic twins discordant for ovarian failure. N Engl J Med 2007; 356:1382–1384.
12. Vanhoutte L, Cortvrindt R, Nogueira D, Smitz J. Effects of chilling on structural aspects of early preantral mouse follicles. Biol Reprod 2004; 70:1041–1048.
13. Hovatta O. Methods for cryopreservation of human ovarian tissue. Reprod Biomed Online 2005; 10:729–734.
14. Kagawa N, Silber S, Kuwayama M. Successful vitrification of bovine and human ovarian tissue. Reprod Biomed Online 2009; 18:568–577.
15. dela Pena EC, Takahashi Y, Katagiri S, Atabay EC, Nagano M. Birth of pups after transfer of mouse embryos derived from vitrified preantral follicles. Reproduction 2002; 123:593–600.
16. Carroll J, Whittingham DG, Wood MJ, Telfer E, Gosden RG. Extra-ovarian production of mature viable mouse oocytes from frozen primary follicles. J Reprod Fertil 1990; 90:321–327.
17. Cortvrindt R, Smitz J, Van Steirteghem AC. A morphological and functional study of the effect of slow freezing followed by complete in-vitro maturation of primary mouse ovarian follicles. Hum Reprod 1996; 11:2648–2655.
18. Cortvrindt R, Smitz J, Van Steirteghem AC. In-vitro maturation, fertilization and embryo development of immature oocytes from early preantral follicles from prepubertal mice in a simplified culture system. Hum Reprod 1996; 11:2656–2666.
19. Carroll J, Whittingham DG, Wood MJ. Growth in vitro and acquisition of meiotic competence after the cryopreservation of isolated mouse primary ovarian follicles. Reprod Fertil Dev 1991; 3:593–599.
20. Nayudu PL, Osborn SM. Factors influencing the rate of preantral and antral growth of mouse ovarian follicles in vitro. J Reprod Fertil 1992; 95:349–362.
21. Xu M, Kreeger PK, Shea LD, Woodruff TK. Tissue-engineered follicles produce live, fertile offspring. Tissue Eng 2006; 12:2739–2746.
22. Xu M, West-Farrell ER, Stouffer RL, Shea LD, Woodruff TK, Zelinski MB. Encapsulated three-dimensional culture supports development of nonhuman primate secondary follicles. Biol Reprod 2009; 81:587–594.
23. Xu M, Barrett SL, West-Farrell E, Kondapalli LA, Kiesewetter SE, Shea LD, Woodruff TK. In vitro grown human ovarian follicles from cancer patients support oocyte growth. Hum Reprod 2009; 24:2531–2540.
24. Moon JH, Hyun CS, Lee SW, Son WY, Yoon SH, Lim JH. Visualization of the metaphase II meiotic spindle in living human oocytes using the Polscope enables the prediction of embryonic developmental competence after ICSI. Hum Reprod 2003; 18:817–820.
25. Rienzi L, Ubaldi F, Martinez F, Iacobelli M, Minasi MG, Ferrero S, Tesarik J, Greco E. Relationship between meiotic spindle location with regard to the polar body position and oocyte developmental potential after ICSI. Hum Reprod 2003; 18:1289–1293.
26. Rienzi L, Ubaldi F, Iacobelli M, Minasi MG, Romano S, Greco E. Meiotic spindle visualization in living human oocytes. Reprod Biomed Online 2005; 10:192–198.
27. Liu L, Oldenbourg R, Trimarchi JR, Keefe DL. A reliable, noninvasive technique for spindle imaging and enucleation of mammalian oocytes. Nat Biotechnol 2000; 18:223–225.
28. Keefe D, Tran P, Pellegrini C, Oldenbourg R. Polarized light microscopy and digital image processing identify a multilaminar structure of the hamster zona pellucida. Hum Reprod 1997; 12:1250–1252.
29. Colonna R, Mangia F. Mechanisms of amino acid uptake in cumulus-enclosed mouse oocytes. Biol Reprod 1983; 28:797–803.
30. Haghighat N, Van Winkle LJ. Developmental change in follicular cell-enhanced amino acid uptake into mouse oocytes that depends on intact gap junctions and transport system Gly. J Exp Zool 1990; 253:71–82.
31. Sela-Abramovich S, Edry I, Galiani D, Nevo N, Dekel N. Disruption of gap junctional communication within the ovarian follicle induces oocyte maturation. Endocrinology 2006; 147:2280–2286.
32. Furger C, Cronier L, Poirot C, Pouchelet M. Human granulosa cells in culture exhibit functional cyclic AMP-regulated gap junctions. Mol Hum Reprod 1996; 2:541–548.
33. Saito T, Hiroi M, Kato T. Development of glucose utilization studied in single oocytes and preimplantation embryos from mice. Biol Reprod 1994; 50:266–270.
34. Johnson MT, Freeman EA, Gardner DK, Hunt PA. Oxidative metabolism of pyruvate is required for meiotic maturation of murine oocytes in vivo. Biol Reprod 2007; 77:2–8.
35. Anderson E, Albertini DF. Gap junctions between the oocyte and companion follicle cells in the mammalian ovary. J Cell Biol 1976; 71:680–686.
36. Carabatsos MJ, Elvin J, Matzuk MM, Albertini DF. Characterization of oocyte and follicle development in growth differentiation factor-9-deficient mice. Dev Biol 1998; 204:373–384.
37. Kreeger PK, Deck JW, Woodruff TK, Shea LD. The in vitro regulation of ovarian follicle development using alginate-extracellular matrix gels. Biomaterials 2006; 27:714–723.
38. Barrett SL, Albertini DF. Allocation of gamma-tubulin between oocyte cortex and meiotic spindle influences asymmetric cytokinesis in the mouse oocyte. Biol Reprod 2007; 76:949–957.
39. Oldenbourg R. A new view on polarization microscopy. Nature 1996; 381:811–812.
40. Gershon E, Plaks V, Aharon I, Galiani D, Reizel Y, Sela-Abramovich S, Granot I, Winterhager E, Dekel N. Oocyte-directed depletion of connexin43 using the Cre-LoxP system leads to subfertility in female mice. Dev Biol 2008; 313:1–12.

41. Luciano AM, Chigioni S, Lodde V, Franciosi F, Luvoni GC, Modina SC. Effect of different cryopreservation protocols on cytoskeleton and gap junction mediated communication integrity in feline germinal vesicle stage oocytes. Cryobiology 2009; 59:90–95.

42. Chi HJ, Koo JJ, Kim MY, Joo JY, Chang SS, Chung KS. Cryopreservation of human embryos using ethylene glycol in controlled slow freezing. Hum Reprod 2002; 17:2146–2151.

43. Cocero MJ, Diaz de la Espina SM, Aguilar B. Ultrastructural characteristics of fresh and frozen-thawed ovine embryos using two cryoprotectants. Biol Reprod 2002; 66:1244–1258.

44. Keros V, Xella S, Hultenby K, Pettersson K, Sheikhi M, Volpe A, Hreinsson J, Hovatta O. Vitrification versus controlled-rate freezing in cryopreservation of human ovarian tissue. Hum Reprod 2009; 24:1670–1683.

45. Mazur P, Seki S, Pinn IL, Kleinhans FW, Edashige K. Extra- and intracellular ice formation in mouse oocytes. Cryobiology 2005; 51:29–53.

46. Barrett SL, Albertini DF. Cumulus cell contact during oocyte maturation in mice regulates meiotic spindle positioning and enhances developmental competence. J Assist Reprod Genet 2010; 27:29–39.

47. Songsasen N, Yu IJ, Ratterree MS, VandeVoort CA, Leibo SP. Effect of chilling on the organization of tubulin and chromosomes in rhesus monkey oocytes. Fertil Steril 2002; 77:818–825.

48. Sathananthan AH, Kirby C, Trounson A, Philipatos D, Shaw J. The effects of cooling mouse oocytes. J Assist Reprod Genet 1992; 9:139–148.

49. Bernard A, Fuller BJ. Cryopreservation of human oocytes: a review of current problems and perspectives. Hum Reprod Update 1996; 2:193–207.

50. Eroglu A, Toner M, Leykin L, Toth TL. Cytoskeleton and polyploidy after maturation and fertilization of cryopreserved germinal vesicle-stage mouse oocytes. J Assist Reprod Genet 1998; 15:447–454.

51. De Santis L, Cino I, Rabellotti E, Calzi F, Persico P, Borini A, Coticchio G. Polar body morphology and spindle imaging as predictors of oocyte quality. Reprod Biomed Online 2005; 11:36–42.

52. Wang Q, Sun QY. Evaluation of oocyte quality: morphological, cellular and molecular predictors. Reprod Fertil Dev 2007; 19:1–12.

53. Wang WH, Keefe DL. Spindle observation in living mammalian oocytes with the polarization microscope and its practical use. Cloning Stem Cells 2002; 4:269–276.

54. Katoh K, Langford G, Hammar K, Smith PJ, Oldenbourg R. Actin bundles in neuronal growth cone observed with the Pol-Scope. Biol Bull 1997; 193:219–220.

55. Navarro PA, Liu L, Trimarchi JR, Ferriani RA, Keefe DL. Noninvasive imaging of spindle dynamics during mammalian oocyte activation. Fertil Steril 2005; 83(suppl 1):1197–1205.